NRL Report 7270

The Influence of Geometric Variables on K_c Values for Two Thin Sheet Aluminum Alloys

A. M. SULLIVAN AND C. N. FREED

Strength of Metals Branch
Metallurgy Division

June 17, 1971

NAVAL RESEARCH LABORATORY
Washington, D.C.

Security Classification

DOCUMENT CONTROL DATA - R & D

(Security classification of title, body of abstract and indexing annotation must be entered when the overall report is classified)

1. ORIGINATING ACTIVITY (Corporate author)	2a. REPORT SECURITY CLASSIFICATION
Naval Research Laboratory Washington, D.C. 20390	Unclassified
	2b. GROUP

3. REPORT TITLE

THE INFLUENCE OF GEOMETRIC VARIABLES ON K_c VALUES FOR TWO THIN SHEET ALUMINUM ALLOYS

4. DESCRIPTIVE NOTES (Type of report and inclusive dates)

This report completes one phase of a continuing problem.

5. AUTHOR(S) (First name, middle initial, last name)

Sullivan, Anna M., and Freed, Charles N.

6. REPORT DATE	7a. TOTAL NO. OF PAGES	7b. NO. OF REFS
June 17, 1971	23	17

8a. CONTRACT OR GRANT NO.	9a. ORIGINATOR'S REPORT NUMBER(S)
NRL Problem M01-24 b. PROJECT NO. Project RR 007-01-46-5431 c. d.	NRL Report 7270 9b. OTHER REPORT NO(S) (Any other numbers that may be assigned this report)

10. DISTRIBUTION STATEMENT

Approved for public release; distribution unlimited.

11. SUPPLEMENTARY NOTES	12. SPONSORING MILITARY ACTIVITY
	Department of the Navy (Office of Naval Research), Arlington, Va. 22217

13. ABSTRACT

Modern technological applications require the use of high-strength thin sheet materials to take advantage of favorable strength-to-weight ratios. High strength, however, is obtained at the expense of fracture toughness. A low toughness significantly decreases the size of flaws which can be tolerated prior to instability and final catastrophic structural failure.

Linear-elastic fracture mechanics (LEFM) provides an analytical framework to define the relationship between flaw size and stress level by the single parameter K. At instability for thin sheet, this parameter becomes K_c, indicating the critical value for a situation of plane stress. To develop a standardized specimen and test procedures, a program has recently been initiated to explore the variables associated with thin sheet fracture testing.

Utilizing a centrally notched sheet tensile specimen, the ratio of the crack length to sheet width (2a/W) and sheet width W have been studied for two high-strength aluminum alloys. Studies indicated that for a 12-in. (30-cm) wide sheet, values of $0.43 \geq 2a_0/W \geq 0.10$ do not influence the value of $K_c = 55.4$ ksi$\sqrt{\text{in.}}$ (60.8 N/cm^2 $\sqrt{\text{cm}}$) for aluminum alloy 7178-T6. Similarly, for alloy 7075-T6 a value of $K_c = 65.2$ ksi$\sqrt{\text{in.}}$ (71.4 N/cm^2 $\sqrt{\text{cm}}$) is obtained between $0.50 \geq 2a_0/W \geq 0.066$. Further, for these two materials, specimen widths of 3, 6, 9, 12 in. (7.5, 15, 23, and 30 cm) give constant values of K_c.

DD FORM 1 NOV 65 1473 (PAGE 1)

S/N 0101-807-6801

Security Classification

14. KEY WORDS	LINK A		LINK B		LINK C	
	ROLE	WT	ROLE	WT	ROLE	WT
High-strength alloy sheet material						
Fracture mechanics						
Fracture toughness						
Fracture test procedures						
Geometric test variables						
Plane stress K_c						
Instability						
Critical flaw size and stress level						

CONTENTS

ABSTRACT

Modern technological applications require the use of high-strength thin sheet materials to take advantage of favorable strength-to-weight ratios. High strength, however, is obtained at the expense of fracture toughness. A low toughness significantly decreases the size of flaws which can be tolerated prior to instability and final catastrophic structural failure.

Linear-elastic fracture mechanics (LEFM) provides an analytical framework to define the relationship between flaw size and stress level by the single parameter K. At instability for thin sheet, this parameter becomes K_c, indicating the critical value for a situation of plane stress. To develop a standardized specimen and test procedures, a program has recently been initiated to explore the variables associated with thin sheet fracture testing.

Utilizing a centrally notched sheet tensile specimen, the ratio of crack length to sheet width (2a/W) and sheet width W have been studied for two high-strength aluminum alloys. Studies indicated that for a 12-in. (30-cm) wide sheet, values of $0.43 \geq 2a_0/W \geq 0.10$ do not influence the value of K_c = 55.4 ksi $\sqrt{\text{in.}}$ (60.8 N/cm^2 $\sqrt{\text{cm}}$) for aluminum alloy 7178-T6. Similarly, for alloy 7075-T6 a value of K_c = 65.2 ksi $\sqrt{\text{in.}}$ (71.4 N/cm^2 $\sqrt{\text{cm}}$) is obtained between $0.50 \geq 2a_0/W \geq 0.066$. Further, for these two materials, specimen widths of 3, 6, 9, and 12 in. (7.5, 15, 23, and 30 cm) give constant values of K_c.

PROBLEM STATUS

This report completes one phase of the problem; work is continuing.

AUTHORIZATION

NRL Problem M01-24
Project RR 007-01-46-5431

Manuscript submitted February 24, 1971.

SYMBOLS

a, a_c, a_0	half-length of crack; subscript c refers to critical value, subscript 0 to initial value
A	cross-sectional area of fracture: Bda
B	specimen thickness
COD	crack opening displacement
E	Young's modulus
$\mathcal{G}$, $\mathcal{G}_c$	strain energy release rate per unit area, crack extension force; subscript c refers to critical value
k	stress concentration factor
ksi	kips per square inch, i.e., $10^3 \times$ psi
K, K_c, K_{Ic}	stress-intensity factor; subscript c refers to critical value, subscript I to first or opening mode
L	specimen length
M	spring constant: COD/P
P	load
r, r_y	distance from crack tip plastic zone; subscript y refers to value at $K_c(K_{Ic})$ and σ_{ys} according to Eq. (4)
T	surface tension
U	elastic strain energy
W, W_{min}	specimen width; subscript min refers to minimum value
W	plastic work
Y	distance of displacement gage from slit
ν	Poisson's ratio
σ_G	gross or nominal stress, P/A
σ_y	normal stress in the y direction
σ_{ys}	yield stress

THE INFLUENCE OF GEOMETRIC VARIABLES ON K_c VALUES FOR TWO THIN SHEET ALUMINUM ALLOYS

INTRODUCTION

The catastrophic collapse of numerous structures over the past decade — high-performance aircraft, missile casings, thin-walled pressure containers — illustrates the reality of the notch brittle fracture problem in structures fabricated from high- and ultrahigh-strength sheet metal alloys. The low fracture resistance of these materials provides for the occurrence of fracture at nominally elastic stress levels when a notch or sharp crack is present. A combination of a critical crack length and stress level (load) exists for the material, which if exceeded, will cause the commencement of uncontrollable crack propagation.

The ability of a metal to withstand the deleterious effects of cracks, notches, or flaws is described by a property called fracture toughness. There is at the present time no standardized test to assess this material property in high-strength thin metal sheet. This report describes a test procedure which is being utilized to measure the fracture resistance of high-strength sheets which fail under elastic loads. The test is based on fracture mechanics plane stress (K_c) concepts for definition of critical crack size-vs-stress level conditions for fracture. Thus, the fracture test not only enables the measurement of fracture toughness per se, but the critical crack size-vs-stress level relationships provide for evolving rational fracture-safe design procedures for use of thin metal sheet.

With a systematic approach to the investigation of the complex specimen geometry relationships associated with thin sheet testing, it is projected that a relatively economical K_c test method can be developed for reliable fracture toughness characterization of high- and ultrahigh-strength thin metal sheet.

DEVELOPMENT OF THE CONCEPTS OF FRACTURE MECHANICS

Recognition by Irwin (1) that the Griffith Energy Balance (2) concept could be related to unstable crack propagation in a ductile material was the keystone of that discipline now known as Linear Elastic Fracture Mechanics (LEFM).

The stability conditions for a crack in a loaded structure may be expressed as

$$\frac{dU}{dA} + \frac{dW}{dA} = 0, \tag{1}$$

where A is area. However, here the term dW/dA is no longer considered as the theoretical surface tension 2T but is defined as the total work per unit area of crack extension. It is seen that while changes in stored elastic energy U and work W rates are balanced, a crack may grow slowly, but when the release of elastic energy becomes excessive, uncontrollable fracture will result.

To prove this relationship, expressed by Eq. (1), initial attempts were made to measure both quantities. Largely, however, efforts were directed to explain velocity effects

in fracturing by Mott's adaptation of the Griffith expression (3). Early work was done using primarily beam specimens; however, the use of sheet specimens was also investigated. For both types of specimens, the breaking stress could be readily determined. However, measurement of the final crack length was a difficult problem since finite slow crack growth frequently preceded instability. Attempts to delineate the crack length at instability by ink-staining techniques met with indifferent success. Further, the introduction of the staining fluid provided an adverse environment so the potential for stress-corrosion-crack growth also existed.

Gradual improvement of experimental techniques and a more fundamental understanding of the implications of the relationship, Eq. (1), produced the familiar expression for $\mathcal{J}$ defined then as the rate of release of elastic energy but essentially measured as work rate (4,5);

$$\mathcal{J} = \frac{dW}{Bda} = E\,\sigma_G^2 W\,\frac{d(1/M)}{d(a/W)}\,. \tag{2}$$

Here E is Young's modulus; σ_G, gross stress on the specimen; B, thickness; W, width; and a, crack length; while 1/M is compliance, which is crack opening displacement (COD) divided by σW. The critical value of $\mathcal{J}$, that of instability at the onset of uncontrollable fracture, was distinguished as $\mathcal{J}_c$.

Given this equation, a calibration curve of COD vs crack length could be developed by elastically loading specimens featuring increasing slit lengths to give values of the spring constant. Plotted as the normalized value $E[COD]/\sigma W$ against 2a/W, instantaneous crack lengths could now be determined for the growing crack from spring constants measured at appropriate intervals along the load-vs-displacement curve. Also, the curve of 1/M vs a/W could be graphically differentiated and thus values of $\mathcal{J}$ computed from the known stress σ_G and crack length 2a. Since the relationship would be true regardless of specimen configuration, all types of specimens, and even structures, could be analyzed in a similar manner.

While these load-vs-crack length relationships were being investigated, another known fact was not ignored — the existence of a stress field at the crack tip. Briefly, it can be stated that away from the leading edge of a crack

$$\sigma_y = \frac{K}{\sqrt{2\pi r}}, \tag{3}$$

where σ_y is the normal stress in the y direction; K, some constant; and r, distance from the crack tip. K is obviously a stress-intensification factor with analogies to the stress-concentration factor "k" of Neuber (6).

It is obvious that σ_y cannot become infinite in a real material with yield stress σ_{ys}, as the metal at the crack tip will yield when $\sigma_y = \sigma_{ys}$ with consequent plastic deformation over a finite region. Rewriting the expression with this in mind, we have

$$\sigma_{ys} = \frac{K_c}{\sqrt{2\pi r_y}}, \tag{4}$$

where K_c is the critical stress-intensity factor and r_y is the radius of the crack-tip plastic zone. The relationship between K_c and $E\mathcal{J}$

$$E\,\mathcal{J}_c = K_c^2 \tag{5}$$

is discussed by Irwin (7).

Theoretical analytic solutions exist which describe the stress field around a crack for several specific specimen configurations, and these can be used advantageously in assigning an expression for the evaluation of K. Refinements in these expressions are still under development and are discussed in Ref. 8.

With the establishment of the foregoing relationships, real tools were now available for the study of fracture. These basic equations (2, 3, 4, and 5) permitted estimates of crack length and calculations of the critical values δ_c and K_c. The values so determined could be used for design purposes to postulate critical load-bearing capacity in the presence of a crack of known length or, alternately, the crack length which could be tolerated under a known load. Progress was not rapid in the field of LEFM, particularly in the exploitation of its practical applications.

GEOMETRICAL DEPENDENCIES OF K_c

During the initial development of fracture mechanics, inasmuch as specimen dimensions were part of the basic equations, it was tacitly assumed that these would be self-normalizing. Theoretically then, instability could be determined from small specimens and would not be dependent on geometry. Implicit also was the feeling that the value obtained for δ_c would reflect a plane stress situation.

It soon became obvious that, although not predicted by the theory, specimen dimensions did influence the fracture toughness values. The dependence on specimen geometry was greatly minimized in the testing of thick sections which are subject to a plane-strain stress state. Consequently, the effort to develop a fracture mechanics test was directed toward high-strength, thick-section plate material. In 1968, a tentative test method for thick-section, plane-strain metals was accepted by ASTM for use pending its adoption as a standard test (9).

Development of this test method has enabled researchers to return to the more difficult problem of characterizing the fracture resistance of thin sheet. The analytic tools and experimental procedures made available in the thick-section effort can be applied to the thin sheet problem. However, unlike the plane-strain test in which specimen variables are minimized, the thin-section, plane-stress test must contend with the dependence of the specimen geometry on the fracture-resistance value. The K_c value is dependent upon sheet thickness, specimen width, initial crack length, and the width-to-length ratio of the test panel. Previous work (10-13) and the results of investigations described in this report indicate that the influence of specimen width, length-to-width ratio, and crack length on the K_c value can be predicted. By employment of judicious specimen design, the effect of these variables on the fracture toughness can be minimized, leaving thickness as the only variable which will significantly affect K_c.

TEST PROCEDURE

A variety of specimen configurations can be utilized for the assessment of fracture toughness; not all, however, are applicable to thin sheet material. The centrally slotted tensile sheet has been chosen for initial experimental work. Of simple design, several mathematical stress analyses of this specimen have been conducted with excellent agreement (8). Because unstable fracture does occur in this specimen, it seemed a more natural structural prototype precursor than the crack-line loaded specimen in current use in other laboratories.

Figure 1 indicates the configuration of this specimen. The central slit was produced by an electric discharge method. While the specimen is loaded in tension, load and crack

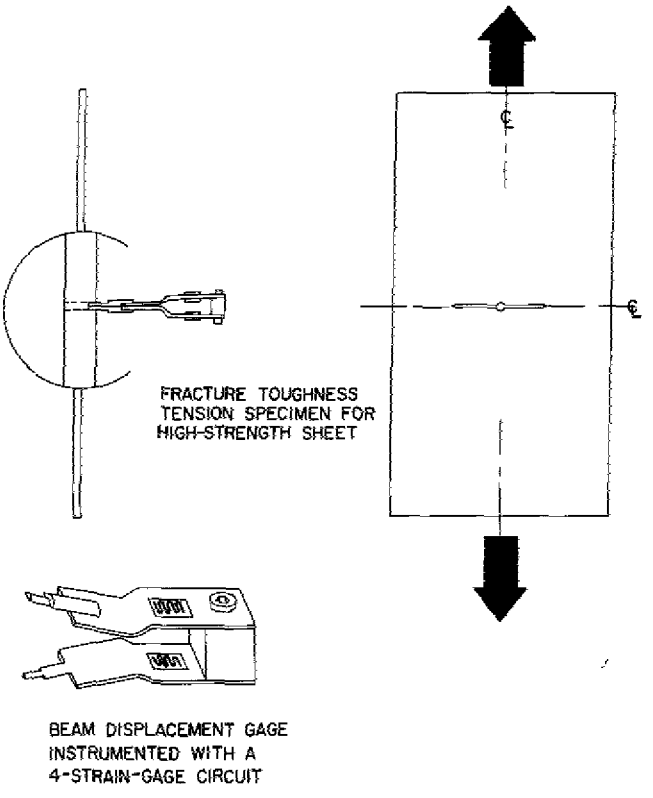

Fig. 1 - Center-notched sheet (CNS) specimen with drawing of displacement gage

opening (COD) are simultaneously graphed by a Mosely X-Y recorder until the specimen fails. To calculate K_c using the appropriate equation (Eq. (8)) requires a knowledge of gross stress σ_G and crack length, 2a, since

$$K_c = \sigma_G \sqrt{a_c}\, f(2a/W), \tag{6}$$

where for a range of 2a/W between 0 and 0.6 the following expression is accurate to within 1 percent:

$$f(2a/W) = 1.77\left[1 - 0.1(2a/W) + (2a/W)^2\right]. \tag{7}$$

Appendix A discusses at length the calibration procedure employed to convert COD measurements to instantaneous crack length.

Variations in $2a_0/W$ and W were investigated to determine the limits of geometrical dependency. As these may vary with K_c/σ_{ys} ratio, results obtained at present are not considered of general applicability.

It should further be noted that, although an extension of the initial slot by fatiguing is desirable to produce a "natural" sharp crack tip, it is unnecessary when some crack growth precedes final fracture (14). The specimens prepared for this report were not fatigued, but the majority evidenced some slow crack growth.

MATERIALS

The two high-strength aluminum alloys 7178-T6 and 7075-T6 were investigated. Table 1 details their mechanical properties.

Table 1

Alloys	Yield Strength* σ_{ys} (ksi)	Tensile Strength σ_{UTS} (ksi)	Elongation in 2-in. (%)
7178-T6	78.9	88.6	9.2
7075-T6	76.5	88.6	10.8

*Offset + 0.2 percent.

DISCUSSION OF EXPERIMENTAL RESULTS

Values obtained for K_c from sheet specimens containing varied initial crack lengths are shown in Figs. 2 and 3, wherein K_c is plotted against 2a/W.

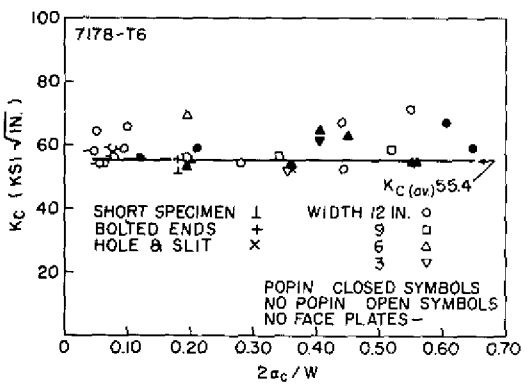

Fig. 2 - Relationship between K_c and 2a/W for 7178-T6 aluminum; K_c = 55.4 ksi $\sqrt{in.}$

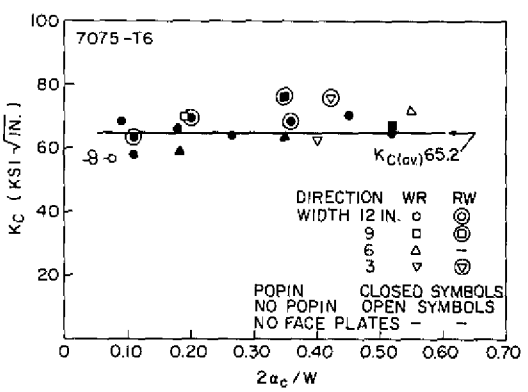

Fig. 3 - Relationship between K_c and 2a/W for 7075-T6 aluminum; K_c = 65.2 ksi $\sqrt{in.}$

The necessity of normalizing the crack length with the width arises from the fact that the basic equation (Eq. (6)) includes a width correction term, $f(2a/W)$. Included also are data from varied specimen widths: 3, 6, 9, and 12 in. (7.5, 15, 22.5, and 30 cm). The majority of tests were made in the WR specimen fracture orientation considered as representing the most unfavorable condition. The few tests in the RW direction (for 7075-T6) perhaps indicate a slight improvement in toughness. Otherwise, those specimens exhibiting "popin," i.e., short, abrupt crack extension with no load increase, give values of K_c within ±10 percent—a reasonable scatter using present techniques. Elimination of the buckling restraints for very short crack lengths shows little effect.

Consideration of (a) material scarcity and (b) difficulties inherent in the heat treatment of thin stock indicated that minimizing specimen length would be a practical necessity. Accordingly, several foreshortened specimens (L = 28 in., 70 cm) of 7178-T6 were

tested as indicated. The "bolted" specimen so designated was a 12-in. (30-cm) long center section bolted to two 12-in. (30-cm) long end tabs. K_c values consistent with those measured using longer specimens support Forman's conclusion that a ratio of specimen length to crack length (L/a) equal to 3 is sufficient (11).

These curves indicate that valid K_c data are produced for these alloys in specimens as narrow as 3 in. (7.5 cm) and between ranges for 7178-T6 of $0.43 \geq 2a/W \geq 0.10$ and for 7075-T6 $0.50 \geq 2a/W \geq 0.066$. The effect of width upon K_c is more clearly seen in Figs. 4 and 5.

The possibility of obtaining the plane strain value K_{Ic} from the popin phenomenon has been exploited (8). Such values for these specimens would not be considered valid, as the initial slits were not extended by fatigue cracks. It is interesting to note, nonetheless, in Figs. 6 and 7, that although $K_{initial}$ values are higher than those reported as K_{Ic} for these materials, reasonable consistency is observed—a fact possibly related to the particular crack-tip radius.

Examination of the stress-to-crack-length relationship, σ_G vs 2a/W, is also informative. Figures 8 and 9 show data points on the theoretical curves computed from the basic K_c equation. In Fig. 9, the data obtained from sheets without buckling restraints indicate a gross stress at fracture lower than expected.

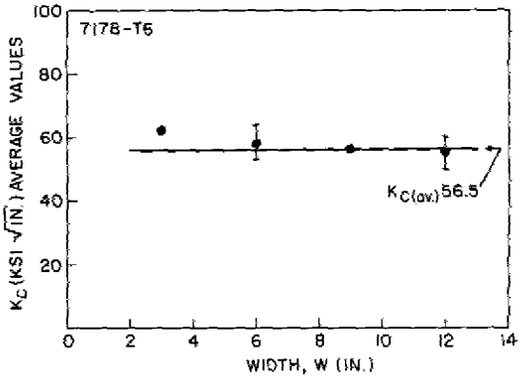

Fig. 4 - Average K_c values plotted for specimens of different widths; 7178-T6, K_c = 56.5

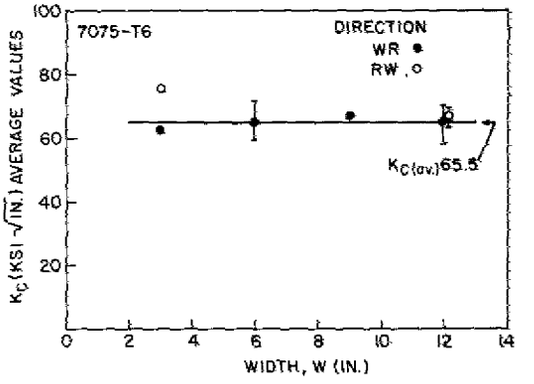

Fig. 5 - Average K_c values plotted for specimens of different widths; 7075-T6, K_c = 65.5

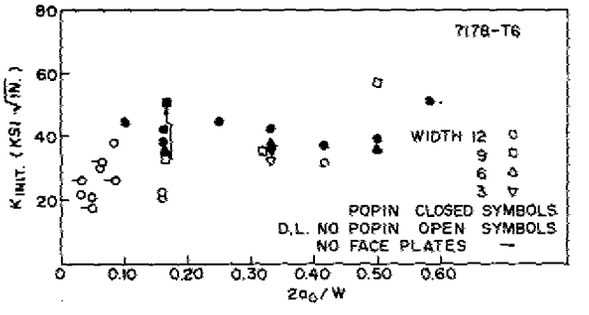

Fig. 6 - K at crack-growth initiation plotted against 2a/W for 7178-T6

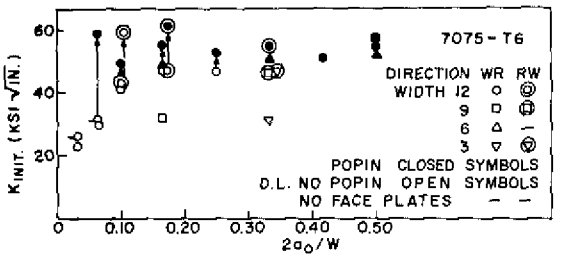

Fig. 7 - K at crack-growth initiation plotted against 2a/W for 7075-T6

Fig. 8 - Stress at fracture σ_G plotted on the theoretical curve ($\sigma_G = K_c/\sqrt{a}$ f 2a/W) at the experimental value of 2a/W for 7178-T6

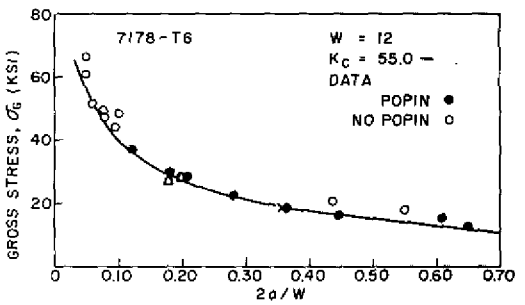

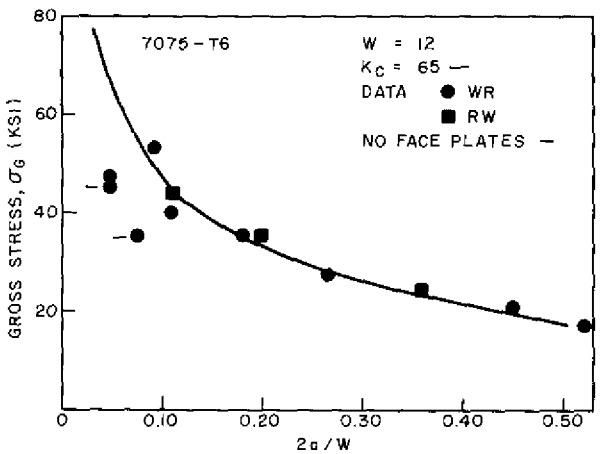

Fig. 9 - Stress at fracture σ_G plotted on the theoretical curve at the experimental values of 2a/W for 7075-T6

CONSIDERATIONS OF MINIMUM SPECIMEN WIDTH

The effect of the dimensional-width variable mentioned earlier is more obvious when the stress-crack length data are compared with those obtained from the infinite sheet expression,

$$K = \sigma_G \sqrt{a} \sqrt{\pi}. \tag{8}$$

This is done in Figs. 10 and 11, where stresses below those postulated from Eq. (8) are observed for the longer crack lengths in specimens of finite width. Straight-line tangents to these curves are drawn in accordance with Fedderson's specifications (15). He concluded, after analyzing a large body of data from diverse sources, that in plots such as these, tangents to certain points would assist in the predication of both expected failure stress and minimum allowable specimen width.

For example, consider a specimen 12-in. (30 cm) wide. From the value of 2a = W = 12, a tangent is constructed to the theoretical curve for an infinite sheet. Then, along this tangent line, failure stress values will fall when the crack length exceeds the value marked by the position of tangency. It was noted that, for the data available, this position corresponded approximately to 2a = W/3. Similar tangents have been constructed for the other specimen widths tested, 3, 6, and 9 in. (7.5, 15, and 22.5 cm). Data points tend to fall on the appropriate connecting lines.

Still another inference can be developed from these plots. A line connecting the material yield-stress value with the value of 2a = W will represent the net section stress on the specimen at each crack length. For the 12-in.-wide specimen, much of the theoretical curve lies beneath the σ_N line. However, as specimen width is reduced (lines not drawn in), this σ_N line approaches closer and closer to the curve. If this line is so drawn that it is just tangent to the curve, its projection to the 2a = W abscissa will identify the minimum test-specimen width utilizable and the singular value of 2a for this width. The stress value observed for this minimum-width line was observed to be about two-thirds of the yield-stress value.

A mathematical verification of the tangent defining the minimum sheet width seemed possible and is presented here. The point of tangency of this straight line with the infinite sheet equation identifies the crack length at which the net section stress on the specimen is equal to the yield stress. Now

$$K_c = \sigma_G \sqrt{\pi a} \tag{8a}$$

and

$$\sigma_G = K_c/\sqrt{\pi a}.$$

When K_c is constant, the above expression can be differentiated, as

$$\frac{d\sigma_G}{da} = \frac{K_c}{2\sqrt{\pi}\, a^{3/2}} = \frac{K_c}{2\sqrt{\pi a}\, a} \tag{9}$$

$$= \frac{\sigma_G}{2a}.$$

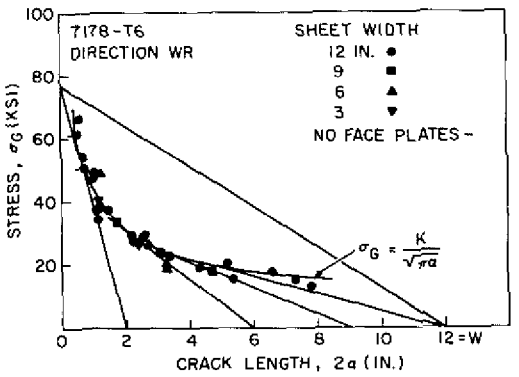

Fig. 10 - Stress at fracture σ_G plotted on the theoretical curve ($\sigma_G = K/\sqrt{\pi a}$) against experimental values of 2a for 7178-T6. Tangents, constructed at values of 2a=W, are explained in the text.

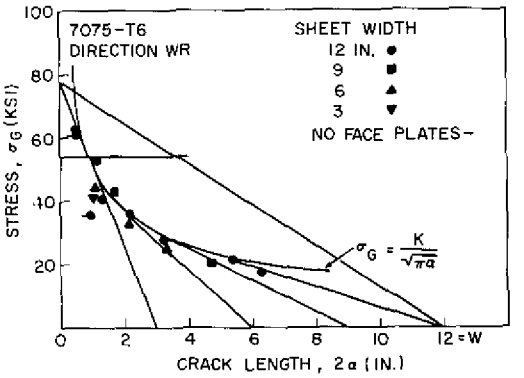

Fig. 11 - Stress at fracture σ_G plotted on the theoretical curve against experimental values of 2a = W for 7075-T6

The equation for the straight line is

$$\sigma_G = \sigma_{ys} + \left(\frac{d\sigma_G}{da}\right) a = \sigma_{ys} - \frac{\sigma_G}{2a} a \,, \tag{10}$$

$$\sigma_G = \sigma_{ys} - \frac{\sigma_G}{2}, \tag{11}$$

$$\text{and } \sigma_{ys} = 1.5\,\sigma_G \text{ or } \sigma_G = 0.66\,\sigma_{ys}. \tag{12}$$

Solving for $a = a_{max}$ when $\sigma_G = 0$ yields

$$a_{max} = \frac{\sigma_{ys}}{d\sigma_G/da} = -\frac{\sigma_{ys}}{\sigma_G/2a} = 2a\,\frac{\sigma_{ys}}{\sigma_G} \tag{13}$$

$$= 2a \times \frac{1.5\sigma_G}{\sigma_G} = 3a;$$

but $a_{max} = W/2$, therefore, at

$$W_{(a\ max)} = 2a_{max} = 2 \times 3a \tag{14}$$

$$= 6a.$$

However, a_{max} is also the minimum width W_{min}. Further, the plastic zone can be evaluated as

$$r_y = \left(\frac{K}{\sigma_{ys}}\right)^2 \frac{1}{2\pi} \tag{15}$$

$$= \left(\frac{\sigma_G\sqrt{\pi a}}{\sigma_{ys}}\right)^2 \frac{1}{2\pi} = \frac{{\sigma_G}^2}{{\sigma_{ys}}^2}\,\frac{\pi a}{2\pi} = \frac{{\sigma_G}^2 a}{2{\sigma_{ys}}^2}. \tag{16}$$

The minimum width can now be stated in terms of r_y, since

$$\sigma_{ys} = 1.5\sigma_G; \quad \therefore \sigma_{ys} = 2.25\ \sigma_G^2$$

$$r_y = \frac{1}{2 \times 2.25} \frac{\sigma_G^2}{\sigma_G^2}\ a = 0.222\ a \tag{17}$$

$$W_{min} = 6a$$

$$\frac{W_{min}}{r_y} = \frac{6a}{0.222a} = 27. \tag{18}$$

The above mathematical development provides a method of estimating minimum specimen width, as follows:

1. σ_{ys} for the material can be known
2. $\sigma_G = 2/3\ \sigma_{ys}$
3. Estimating K_c, $a = \left(K/\sigma_G\right)^2\ 1/\pi = \left(3K/2\sigma_{ys}\right)^2\ 1/\pi$
4. $W_{min} = 6a$
5. $W_{min}/r_y = 27.$

The weak step in this analysis is the necessity of estimating K_c. In general K_c is roughly inversely proportional to σ_{ys}. There are indications in the aluminum alloy data that $K_c \cdot \sigma_{ys}$ may be a constant value for a particular sheet thickness. If this is indeed so, once established, these constants should permit reasonable estimates of K_c from σ_{ys} values; such values can then be used to determine minimum-width values for test verification of the K_c estimate. Until this postulated relationship is established and constants are well defined, it will continue to be necessary to select a range of estimated widths and to test these for constancy of the K_c value. Calculations of W/r_y will also assist in ensuring valid test data, i.e., $W/r_y >> 27$.

To codify this analysis, Table 2 gives calculated and adjusted values of minimum sheet width for different K_c/σ_{ys} ratios, whereas Table 3 indicates expected values of critical crack length at proportionate levels of yield stress.

Table 2
Calculated and Adjusted Values of Minimum Sheet Width and Critical Crack Length for a Valid Test Specimen

K_c/σ_{ys}	W, Calculated	2a (in.)	2a/W	W, Adjusted	2a (in.)	2a/W
0.50	1.08	0.36	0.333	3.0	1.00	0.333
1.00	4.30	1.44	0.333	6.0	2.00	0.333
1.50	9.68	3.22	0.333	12.0	4.00	0.333
2.00	17.20	5.72	0.333	20.0	6.66	0.333
3.00	38.70	12.90	0.333	48.0	16.00	0.333

Table 3
Expected Values of Critical Crack Length
for Different Stress Levels in an Infinite Sheet

K/σ_{ys}	$\sigma_{ys}/2$ 2a (in.)	$3\sigma_{ys}/4$ 2a (in.)	σ_{ys} 2a (in.)
0.50	0.64	0.28	0.16
1.00	2.56	1.12	0.64
1.50	5.76	2.56	1.44
2.00	10.18	4.55	2.56
3.00	23.04	10.24	5.76

CONCLUSIONS

1. K_c determinations can be made for the high-strength aluminum alloys 7178-T6 and 7075-T6, 0.0625-in. (0.156 cm) thick, on specimens 3-in. (7.5-cm) wide.

2. Valid fracture-toughness data are produced over the general range of $0.50 \geq 2a/W \geq 0.10$.

3. Elimination of buckling restraints tends to give lower K_c and σ_G values.

4. Foreshortened specimens, considered for practical reasons, appear to give results consistent with those obtained from longer ones.

5. Mathematical verification of minimum sheet width for various levels of K_c/σ_{ys} ratio is possible. A reasonable estimate of minimum sheet width prior to testing will reduce the number of specimen dimensional variables which must be investigated to ensure valid results.

ACKNOWLEDGMENTS

It is the authors' pleasure to acknowledge the expert assistance of Messrs. S.J. McKaye and R.F. Bryner in the preparation, instrumentation, and conduct of the tests described herein. Appreciation is also expressed to the Office of Naval Research for its financial support of this work.

REFERENCES

1. Irwin, G.R., "Fracture Dynamics," in "Fracturing of Metals," Cleveland:ASM, 147-166, 1947

2. Griffith, A.A., "The Phenomena of Rupture and Flow in Solids," Phil Trans. Roy. Soc. A221:163-198, 1920

3. Mott, N.F., "Slip at Grain Boundaries and Grain Growth in Metals," Proc. Phys. Soc. 60:391, 1948

4. Irwin, G.R., and Kies, J.A., "Fracturing and Fracture Dynamics," Welding J., Res. Suppl. 31:95-100s, 1952

5. Irwin, G.R., and Kies, J.A., "Critical Energy Rate Analysis of Fracture Strength," Welding J., Res. Suppl. 33:193s-198s, 1954

6. Neuber, H., "Kerbspannungslehre," Springer-Verlag, Berlin, 1937

7. Irwin, G.R., "Analysis of Stresses and Strains Near the End of a Crack Traversing a Plate," ASME, J. Appl. Mech. 24:361, 1957

8. Brown, W.F., Jr., and Srawley, J.E., "Plane Strain Crack Toughness Testing of High Strength Metallic Materials," ASTM STP 410, 1966

9. "Tentative Method of Test for Plane Strain Fracture Toughness of Metallic Materials," E-399-70T, Annual Book of ASTM Standards, Part 31, p. 911, 1968

10. Carman, C.M., Armiento, D.F., and Marcus, H., "Crack Resistance Properties of High Strength Aluminum Alloys," Proc. First Int. Conf. on Fracture (Sendai, Japan) 2:995-1038, 1966

11. Kaufman, J.G., and Holt, M., "Fracture Characteristics of Aluminum Alloys," Alcoa Research Laboratory Technical Paper No. 18, New Kensington, Pa., 1965

12. Forman, R.G., "Experimental Program to Determine Effect of Crack Buckling and Specimen Dimensions on Fracture Toughness of Thin Sheet Materials," AF Flight Dynamics Lab., Technical Report AFFDL - TR-65-146, Wright-Patterson AFB, Ohio, 1966

13. Srawley, J.E., and Brown, W.F., Jr., "Fracture Toughness Testing Methods," in "Fracture Toughness Testing and Its Applications," ASTM STP 381, 133-245, 1965

14. Broek, D., "The Residual Strength of Aluminum Alloy Sheet Specimens Containing Fatigue Cracks or Saw Cuts," National Aerospace Laboratory (Amsterdam) Technical Report NLR-TR M. 2143, 1966

15. Fedderson, C., "Some Developments in Residual Strength Analysis," Symposium on Damage Tolerance in Aluminum Aircraft, ASTM Annual Meeting in Toronto, 1970

16. Westergaard, H.M., "Bearing Pressures and Cracks," Trans. ASME, J. Appl. Mech., 6:A49-A53, 1939

17. Paris, P.C., and Sih, G.C., "Stress Analysis of Cracks," in "Fracture Toughness Testing and Its Applications," ASTM STP 381, 30-82, 1965

Appendix A

CALIBRATION

To monitor the growing crack by crack-opening displacement (COD) measurements, a calibration against crack length was made. Specimens of 7178-T6 aluminum were prepared with the following dimensions: length 36 in. (91 cm); width 12 in. (30 cm); thickness 0.063 in. (0.16 cm). Initial slits, 0.063 in. (0.16 cm) wide, were prepared by an electric discharge method; slit lengths used for calibration were 1.2, 2, 3, 4, 5, 6, and 7 in. (3, 5, 7.5, 10, 12.5, 15, and 17.5 cm).

When panels containing slits longer than 2 in. (5 cm) were loaded, the specimen manifested a tendency to buckle. This is inadmissible, since it perturbs the stress field at the slit tips in a manner not predicted by the analytic expression employed for computation. Therefore, to suppress buckling, split aluminum face plate, 12 in. (30 cm) long by 2 in. (5 cm) wide by 0.5 in. (1.3 cm) thick, were employed. The faces of the plates were covered with Teflon and the backs were made rigid with an aluminum T-shaped section (Fig. A1).

The COD measurement was effected with a strain-gage-instrumented probe having semicircular tips (Fig. A2) to fit into a 0.188-in. (0.478-cm) hole drilled at the slit center. This permitted positioning the face plates quite close to the slit lip. Signals from the strain-gage circuit were fed into a Mosely X-Y recorder together with those from a microformer attachment to the load train of a Baldwin Universal Testing Machine.

Since theoretical expressions have been proposed both for displacements at the slit center (16) and at positions quite close to the slit tip (7), it seemed expedient to provide calibration data suitable for comparison. For this reason, a series of calibrations was made positioning the probe at the center of the slit (a_0 from the tip) and at alternate positions 0.3, 0.6, and 1.6 in. from the tip. Tracings of the load P vs COD are shown in Figs. A3a, b, c, and d for these various probe positions. Three runs were made for each determination at a load well below that of instability for this material.

Data for the center hole position normalized as $E[COD]/\sigma W = EB[COD]/P$ and plotted against 2a/W are displayed in Fig. A4. These values are seen to agree well with a theoretical curve plotted from the equation

$$\frac{E[COD]}{\sigma W} = 2\left\{\frac{2W}{\pi Y}\cosh^{-1}\left(\frac{\cosh \pi Y/W}{\cos \pi a/W}\right) - \frac{1+\nu}{\left[1+\left(\frac{\sin \pi a/W}{\sinh \pi Y/W}\right)^2\right]^{1/2}} + \nu\right\} Y/W \qquad \text{(A1)}$$

Values selected to test the validity of this expression are W = 12 in.; Y = 0.0625 in.; a = a_0, the successive half slit lengths; π = 3.1416; and ν = 0.33.

Substituting these into Eq. (A1) yields

$$\frac{E[COD]}{\sigma W} = 2\left\{122.2\cosh^{-1}\left(\frac{1.0001}{\cos \pi a/W}\right) - \frac{1.33}{\left[1+\left(\frac{\sin \pi a/W}{0.015}\right)^2\right]^{1/2}} + 0.33\right\} 0.0052. \qquad \text{(A2)}$$

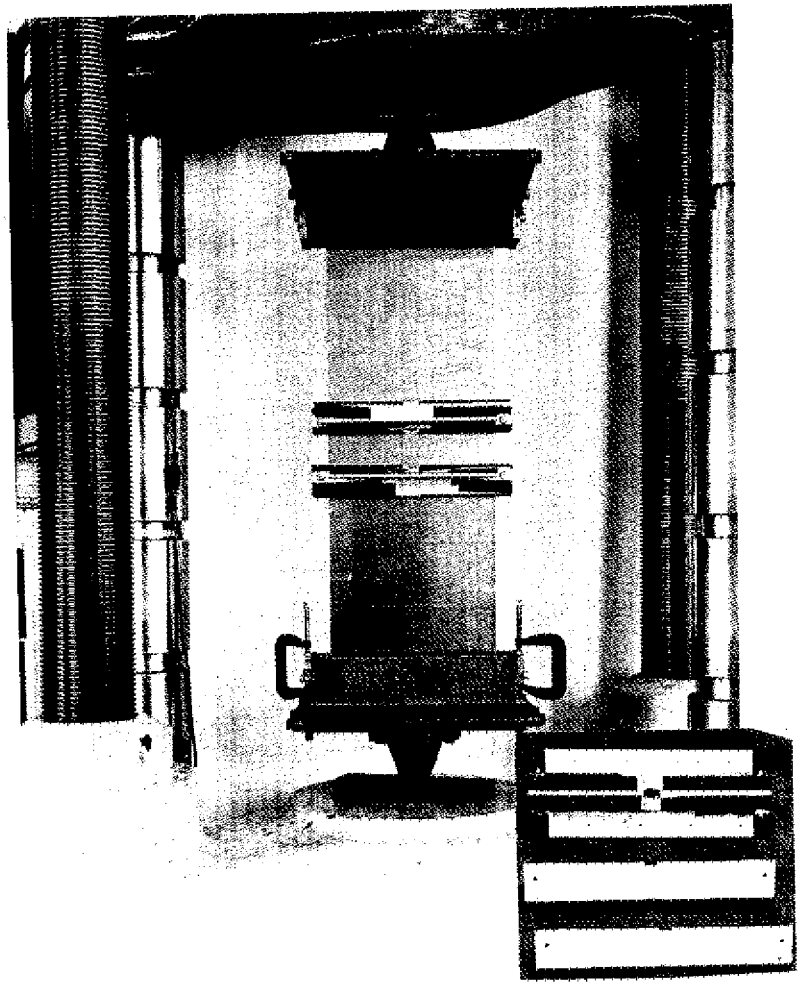

Fig. A1 - Center-notched sheet specimen in testing machine. Face plates attached to the specimen have been moved away from the notch for clarity. The insert at bottom shows details of the face plate more clearly.

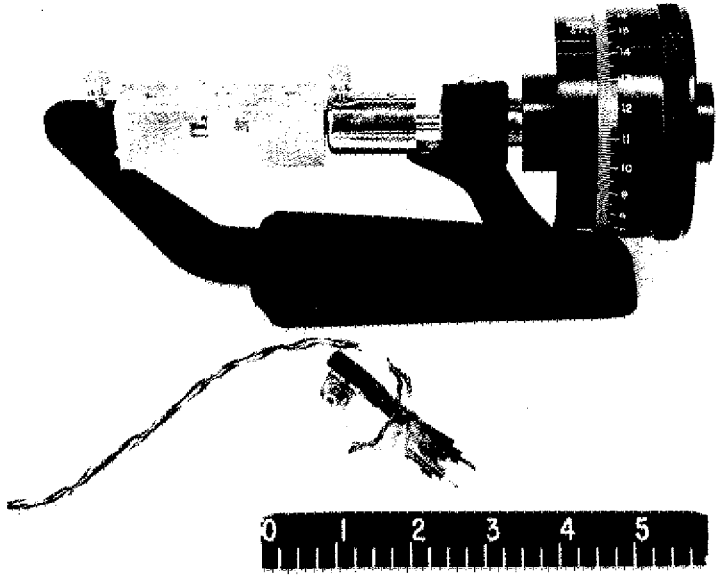

Fig. A2 - Strain-gage-instrumented probe shown together with the instrument used for its calibration

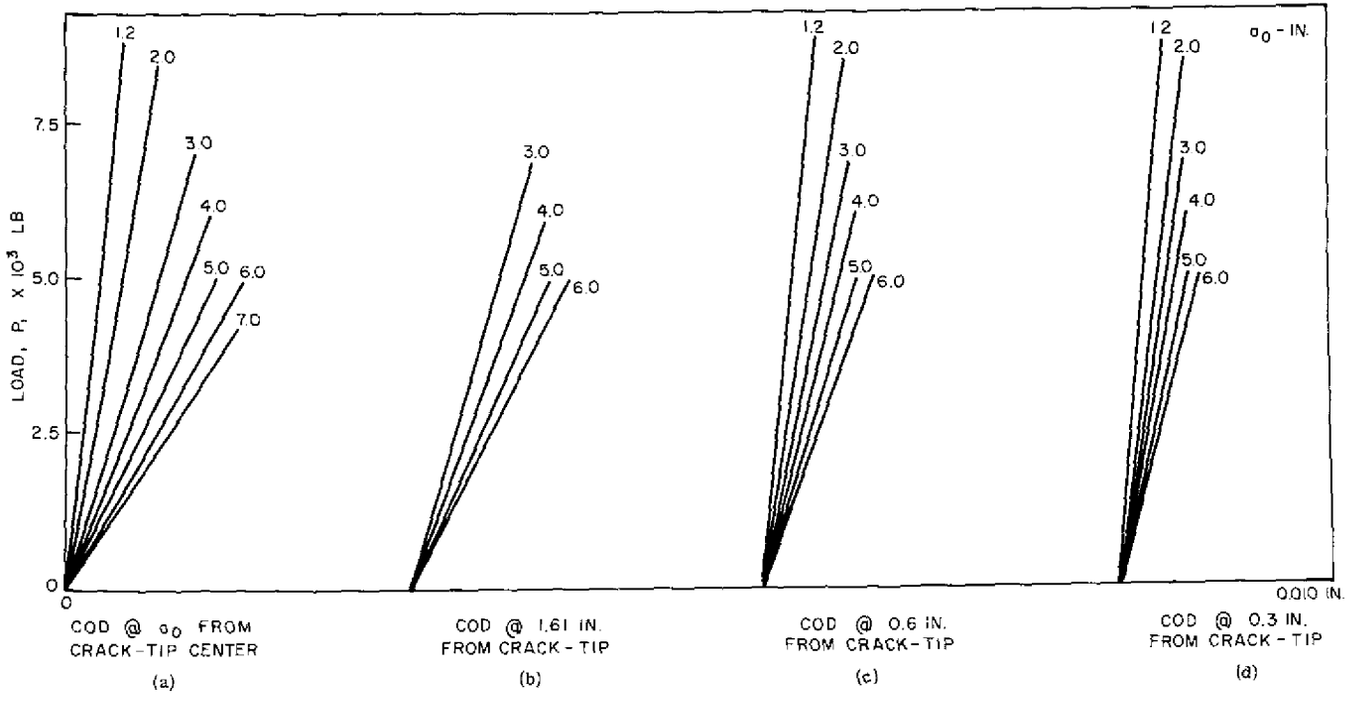

Fig. A3 - Tracings of experimental curves, load vs displacement (P vs COD) for various probe positions

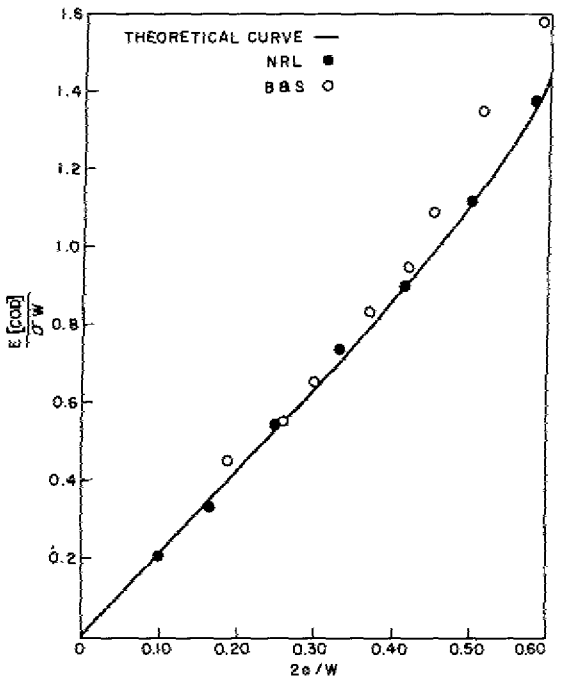

Fig. A4 - Data from Fig. A3a, normalized as $E[COD]/\sigma W$ are plotted on the theoretical curve from Eq. (A1) in Appendix A

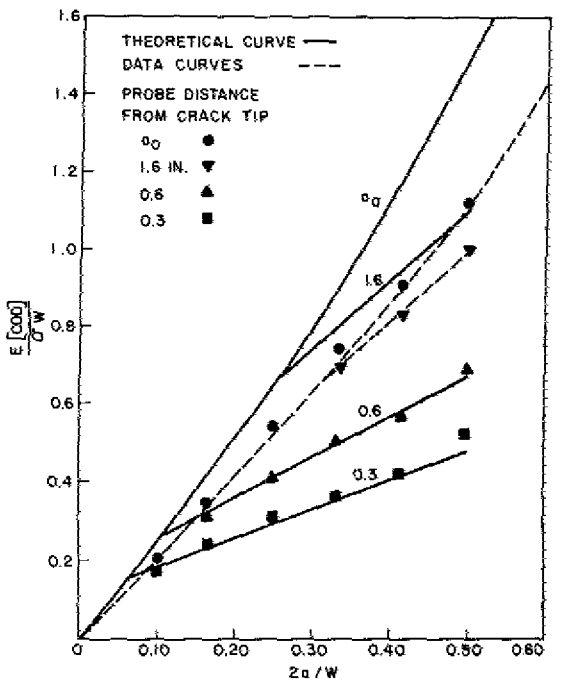

Fig. A5 - All data from Fig. A3, normalized at $E[COD]/\sigma W$, are plotted on the theoretical curves from Eq. (A5) in Appendix A

Because of the close proximity of the probe to the slit, this calibration is now relatively insensitive to specimen width; computed for width values of W = 3 and 12 in., curves are indistinguishable upon plotting. This is not true when Y, the distance of the probe to the slit is 1 in., a position which has frequently been utilized (10).

The other positions of the probe are not suitable for length estimates because as the crack grows the distance from the crack tip continually increases, thus invalidating the calibration curves. However, they do provide a further check on the experimental method employed by comparison with the theoretical estimate proposed by Irwin (7) and further discussed by Paris and Sih (17). Data for all probe hole positions are plotted in Fig. A5, together with theoretical curves from the equation

$$\frac{COD}{2} = \frac{K}{G}(r/2\pi)^{1/2} \sin\frac{\theta}{2}\left[2 - 2\nu - \frac{\cos^2\theta}{2}\right]. \qquad (A3)$$

To normalize this expression, since by definition $K = (P/BW)\sqrt{a}\, f(2a/W)$ for this center-notched sheet specimen, it can be substituted into Eq. (A3) so that

$$COD = \frac{(2P/BW)\sqrt{a}\, f(2a/W)}{G}\left(\frac{r}{2\pi}\right)^{1/2} \sin\frac{\theta}{2}\left[2 - 2\nu - \frac{\cos^2\theta}{2}\right] \qquad (A4)$$

and

$$\frac{E[COD]}{\sigma W} = \frac{2E}{GW}\sqrt{a}\, f(2a/W)\left(\frac{r}{2\pi}\right)^{1/2} \sin\frac{\theta}{2}\left[2 - 2\nu - \frac{\cos^2\theta}{2}\right]. \qquad (A5)$$

Values selected to test the validity of this expression are W = 12 in.; B = 0.0625 in.; $a = a_0$, the successive half-slit lengths; $\pi = 3.1416$; $\nu = 0.33$; $G = 4.4 \times 10^6$ psi; $E = 10.6 \times 10^6$ psi; $\theta = 180°$; and r = successive positions of the probe to the crack tip. Substituting these into Eq. (A5) yields

$$\frac{E[COD]}{\sigma W} = 0.236 \sqrt{r}\ \sqrt{a}\ f(2a/W).$$

The agreement demonstrated for probe positions 0.3 and 0.6 in. from the slit tip is surprising, inasmuch as this model was developed to estimate COD adjacent to the tip.

The comparisons provided in Figs. A4 and A5 serve to ensure confidence in the experimental details (face plates and probe) and the measurement techniques employed. To obtain length estimates of the growing crack, straight lines are drawn from the origin of the load-displacement curve to selected load points. When the slopes are evaluated as COD/P and appropriately normalized (multiply by EB), the value of 2a/W can be read from the calibration curve and thus crack length obtained for known loads. It should be reiterated here that the crack length determined in this manner is considered to be an effective crack length. Its use simplifies computation since the plastic zone correction need not be added to the basic equation for evaluation of K.